


## ORIGINAL ARTICLE

## Obesity Biology and Integrated Physiology

# Hepatic and adipose tissue transcriptome analysis highlights a commonly deregulated autophagic pathway in severe MASLD

Marica Meroni<sup>1</sup> | Emilia De Caro<sup>2</sup> | Federica Chiappori<sup>3</sup> | Miriam Longo<sup>1</sup> |  
 Erika Paolini<sup>1</sup> | Ettore Mosca<sup>3</sup> | Ivan Merelli<sup>3</sup> | Rosa Lombardi<sup>1,4</sup> |  
 Sara Badiali<sup>5</sup> | Marco Maggioni<sup>6</sup> | Alessandro Orro<sup>3</sup> | Alessandra Mezzelani<sup>3</sup> |  
 Luca Valenti<sup>4,7</sup> | Anna Ludovica Fracanzani<sup>1,4</sup> | Paola Dongiovanni<sup>1</sup> 

<sup>1</sup>Medicine and Metabolic Diseases, Fondazione IRCCS Cà Granda Ospedale Maggiore Policlinico, Milan, Italy

<sup>2</sup>Life and Medical Sciences Institute (LIMES), University of Bonn, Germany/System Medicine, German Center for Neurodegenerative Diseases (DZNE), Bonn, Germany

<sup>3</sup>Institute for Biomedical Technologies, National Research Council (ITB-CNR), Segrate, Italy

<sup>4</sup>Department of Pathophysiology and Transplantation, University of Milan, Milan, Italy

<sup>5</sup>Department of Surgery, Fondazione IRCCS Cà Granda Ospedale Maggiore Policlinico, Milan, Italy

<sup>6</sup>Department of Pathology, Fondazione IRCCS Cà Granda Ospedale Maggiore Policlinico, Milan, Italy

<sup>7</sup>Precision Medicine Lab, Biological Resource Center, Department of Transfusion Medicine and Hematology, Fondazione IRCCS Ca' Granda Ospedale Maggiore Policlinico, Milan, Italy

## Correspondence

Paola Dongiovanni, Medicine and Metabolic Diseases, Fondazione IRCCS Cà Granda Ospedale Maggiore Policlinico, Padiglione Quarto, via Pace 9, 20122 Milan, Italy.  
 Email: [paola.dongiovanni@policlinico.mi.it](mailto:paola.dongiovanni@policlinico.mi.it)

## Funding information

Italian Ministry of Health, Grant/Award Numbers: GR-2019-12370172, RF-2021-12374481

## Abstract

**Objective:** The incidence of metabolic dysfunction-associated steatotic liver disease (MASLD) is rapidly ramping up due to the spread of obesity, which is characterized by expanded and dysfunctional visceral adipose tissue (VAT). Previous studies have investigated the hepatic transcriptome across MASLD, whereas few studies have focused on VAT.

**Methods:** We performed RNA sequencing in 167 hepatic samples from patients with obesity and in a subset of 79 matched VAT samples. Circulating cathepsin D (CTSD), a lysosomal protease, was measured by ELISA, whereas the autophagy-lysosomal pathway was assessed by Western blot in hepatic and VAT samples ( $n = 20$ ).

**Results:** Inflammation, extracellular matrix remodeling, and mitochondrial dysfunction were upregulated in severe MASLD in both tissues, whereas autophagy and oxidative phosphorylation were reduced. Tissue comparative analysis revealed 13 deregulated genes, including CTSD, which showed the most robust diagnostic accuracy in discriminating mild and severe MASLD. CTSD expression correlated with circulating protein, whose increase was further validated in 432 histologically characterized MASLD patients, showing a high accuracy in foreseeing severe liver injury. In addition, the assessment of serum CTSD increased the performance of fibrosis 4 in diagnosing advanced disease.

This is an open access article under the terms of the [Creative Commons Attribution-NonCommercial-NoDerivs](https://creativecommons.org/licenses/by-nc-nd/4.0/) License, which permits use and distribution in any medium, provided the original work is properly cited, the use is non-commercial and no modifications or adaptations are made.

© 2024 The Authors. *Obesity* published by Wiley Periodicals LLC on behalf of The Obesity Society.

**Conclusions:** By comparing the hepatic and VAT transcriptome during MASLD, we refined the concept by which CTSD may represent a potential biomarker of severe disease.

## INTRODUCTION

Over the last decades, the prevalence of metabolic dysfunction-associated steatotic liver disease (MASLD) has dramatically increased across different ages and ethnicities, paralleling the escalation of obesity, to the point that it has become the most common chronic liver disease worldwide [1]. Obesity is characterized by expanded visceral adipose tissue (VAT) alongside alterations in its secretory function. Dysfunctional VAT is the most important driver of MASLD to the extent that the latter is present in more than 80% of individuals with obesity [2–4]. As a result of the compromised hormonal activity of VAT, the liver captures circulating fatty acids (FAs) released by adipose tissue, thereby leading to increased hepatic fat accumulation and, in turn, to an inflammatory response, oxidative stress, and autophagy impairment [5, 6]. Collectively, these processes play a key role in the progression from simple steatosis to metabolic dysfunction-associated steatohepatitis (MASH), which may evolve to cirrhosis and hepatocellular carcinoma [7]. Therefore, the strong interaction between liver and VAT, which secretes most of the proteins involved in inflammatory processes and extracellular matrix (ECM) organization, contributes to MASLD pathogenesis and progression, thereby requiring us to face the disease from a multisystemic point of view [8].

The transcriptomic profile has revealed a useful tool to highlight differences in gene expression across the MASLD spectrum. We previously performed bulk RNA sequencing (RNA-seq) in liver samples obtained from 125 individuals with severe obesity and demonstrated that, in advanced MASLD, there was an upregulation of inflammation and a reduced oxidative metabolism. We replicated findings observed in other cohorts with different selection criteria, highlighting the upregulation of, e.g., aldo-keto reductase family 1 member B10 (*AKR1B10*) and growth differentiation factor 15 (*GDF15*) in patients with MASLD with progressive disease, and we identified interleukin-32 (*IL32*) as the most overexpressed gene, whose circulating levels correlated with advanced MASLD [9, 10].

In recent years, an adipocentric perspective of MASLD has emerged, and it is gaining value through the opportunity to restore VAT function for the prevention of severe liver disease. Sheldon et al. performed a complete transcriptomic analysis of VAT from 31 adolescents with severe obesity. They found reduced adipose expansion/remodeling, insulin resistance (IR), inflammation, impaired lipid metabolism, and mitochondrial dysfunction across the MASLD spectrum, thus identifying a tailored adipose tissue RNA signature. However, they missed establishing a cross talk among the

### Study Importance

#### What is already known?

- Obesity represents the main contributor to metabolic dysfunction-associated steatotic liver disease (MASLD), and visceral adipose tissue (VAT) is strongly interlaced with liver in the disease pathogenesis and progression. Although several studies performed hepatic RNA sequencing in patients with MASLD, few studies explored the transcriptomic changes that occur in VAT.

#### What does this study add?

- The novelty of the present study consists in comparing the expression profile of liver and VAT in patients with MASLD to highlight the common mechanisms that connect the increased adiposity with advanced liver injury.
- Therefore, the strong interaction between liver and VAT, which secretes most of the proteins involved in inflammatory processes and extracellular matrix organization, contributes to MASLD progression, thereby requiring us to face the disease from a multisystemic point of view.

#### How might these results change the direction of research or the focus of clinical practice?

- We observed that inflammation and lysosomal autophagy were affected in liver and VAT in severe MASLD, highlighting cathepsin D (CTSD) as a noninvasive biomarker of advanced disease. In addition, we first demonstrated that serum CTSD assessment increased the performance of fibrosis 4 in diagnosing metabolic dysfunction-associated steatohepatitis-fibrosis.

tissues by assessing the expression profile of matched hepatic samples [11].

Therefore, we first aimed to compare the hepatic and VAT transcriptome in 167 patients with obesity and MASLD, stratified according to liver disease severity. We identified a shared gene signature from which circulating cathepsin D (CTSD) emerged as a common biomarker, thus supporting an established key role of the

**TABLE 1** Demographic, anthropometric, and clinical features of 167 patients with severe obesity for whom RNA-seq data were available.

Liver	Hepatic Transcriptomic cohort (n = 167)	Normal liver (n = 29)	Mild MASLD (n = 91)	Severe MASLD (n = 47)	p value
Sex (M/F)	28/139	2/27	9/82	17/30	0.0003*
Age (y)	43 ± 10	42 ± 7.6	43 ± 11	44 ± 9.7	0.49
BMI (kg/m <sup>2</sup> )	41.3 ± 7.4	38 ± 8.7	41 ± 6.3	43.5 ± 7.8	<0.001
IFG/T2D (0/1)	150/17	29/0	82/9	40/8	0.27*
Total cholesterol (mmol/L)	5.3 ± 1.2	5.2 ± 1.4	5.5 ± 1.03	4.9 ± 1.2	0.10
LDL cholesterol (mmol/L)	3.3 ± 0.9	3.5 ± 0.8	3.4 ± 0.8	3.0 ± 1.1	0.09
HDL cholesterol (mmol/L)	1.4 ± 0.35	1.6 ± 0.3	1.4 ± 0.3	1.29 ± 0.4	0.006
Triglycerides (mmol/L)	1.45 ± 0.7	1.1 ± 0.5	1.5 ± 0.7	1.5 ± 0.8	0.07
ALT (IU/L)	16 (20–30)	11 (16–22)	16 (20–26)	23 (31–43)	<0.001
AST (IU/L)	15 (18–24)	14 (16–20)	15 (17–22)	18 (24–31)	<0.001
GGT (IU/L)	15 (24–43)	8 (16–28)	17 (22–46)	27 (36–49)	0.012
Steatosis ≥ 2 (yes), n (%)	82 (49)	0	36 (39)	46 (98)	<0.001*
Lobular inflammation ≥ 1 (yes), n (%)	94 (56)	0	50 (54)	44 (94)	<0.001*
Ballooning ≥ 1 (yes), n (%)	24 (14)	0	3 (3)	21 (45)	<0.001*
NAS > 5 (yes), n (%)	22 (13)	0	0	22 (47)	<0.001*
Fibrosis ≥ 2 (yes), n (%)	13 (8)	0	0	13 (28)	<0.001*
FIB-4	0.72 ± 0.47	0.65 ± 0.23	0.66 ± 0.33	0.89 ± 0.72	0.02
Adipose tissue	Adipose Transcriptomic cohort (n = 79)	Normal liver (n = 16)	Mild MASLD (n = 36)	Severe MASLD (n = 27)	p value
Sex (M/F)	16/63	1/15	5/31	10/17	0.02*
Age (y)	44.1 ± 9.6	44.3 ± 8.2	42.4 ± 10.3	46.3 ± 9.1	0.40
BMI (kg/m <sup>2</sup> )	41.6 ± 7.1	39.9 ± 12.2	41.4 ± 6	42.8 ± 6.4	0.16
IFG/T2D (0/1)	69/10	16/0	33/3	21/7	0.18*
Total cholesterol (mmol/L)	5.2 ± 0.9	5.5 ± 0.95	5.3 ± 0.9	5.2 ± 0.98	0.46
LDL cholesterol (mmol/L)	3.2 ± 0.9	3.4 ± 0.8	3.1 ± 0.8	3.1 ± 1.02	0.71
HDL cholesterol (mmol/L)	1.5 ± 0.35	1.7 ± 0.4	1.4 ± 0.3	1.35 ± 0.4	0.013
Triglycerides (mmol/L)	1.4 ± 0.7	0.95 ± 0.4	1.4 ± 0.6	1.7 ± 0.8	0.010
ALT (IU/L)	21 (16–29)	19 (13–22)	20 (16–23)	29 (18–43)	0.003
AST (IU/L)	19 (16–25)	16 (13–22)	17 (16–22)	23 (18–31)	0.012
GGT (IU/L)	25 (20–43)	21 (14–30)	22 (18–32)	38 (24–50)	0.023
Steatosis ≥ 2 (yes), n (%)	42 (53)	0	15 (42)	27 (100)	<0.001*
Lobular inflammation ≥ 1 (yes), n (%)	50 (63)	0	24 (66)	26 (96)	<0.001*
Ballooning ≥ 1 (yes), n (%)	15 (19)	0	1 (3)	14 (52)	<0.001*
NAS > 5 (yes), n (%)	13 (16)	0	0	13 (48)	<0.001*
Fibrosis ≥ 2 (yes), n (%)	7 (9)	0	0	7 (26)	<0.001*
FIB-4	0.72 ± 0.48	0.57 ± 0.19	0.63 ± 0.22	0.86 ± 0.35	0.002

Note: Values are reported as mean ± SD or median (IQR) as appropriate.

Abbreviations: ALT, alanine aminotransferase; AST, aspartate aminotransferase; F, female; FIB-4, fibrosis 4; GGT, gamma glutamyl transferase; HDL, high-density lipoprotein; IFG, impaired fasting; LDL, low-density lipoprotein; M, male; MASLD, metabolic dysfunction-associated steatotic liver disease; NAS, MASLD activity score; RNA-seq, RNA sequencing; T2D, type 2 diabetes mellitus.

\*p value at  $\chi^2$  test.

autophagy-lysosomal pathway in inducing obesity and MASLD. Then, we confirmed the association between serum CTSD and advanced disease in a validation cohort of 432 histologically characterized MASLD patients and further demonstrated that

assessment of CTSD may improve the diagnostic accuracy of fibrosis 4 (FIB-4), especially for intermediate values. Finally, the autophagy-lysosomal pathway was assessed in liver, VAT, and primary adipocytes from bariatric patients with MASLD.

**TABLE 2** Demographic, anthropometric, and clinical features of 432 patients with MASLD belonging to the validation cohort (Liver Clinic).

Liver	Normal liver (n = 31)	Mild MASLD (n = 231)	Severe MASLD (n = 170)	p value
Sex (M/F)	10/21	139/92	110/60	0.003
Age (y)	40 ± 9.0	48 ± 13	51 ± 12	<0.0001
BMI (kg/m <sup>2</sup> )	36 ± 8.0	32 ± 9.0	33 ± 6.0	0.04
IFG/T2D (0/1)	29/2	197/34	109/61	<0.0001
Total cholesterol (mmol/L)	5.2 ± 0.8	5.2 ± 1.1	4.9 ± 1.0	0.13
LDL cholesterol (mmol/L)	3.4 ± 0.7	3.2 ± 1.0	3.1 ± 1.0	0.33
HDL cholesterol (mmol/L)	1.4 ± 0.4	1.3 ± 0.3	1.2 ± 0.3	0.002
Triglycerides (mmol/L)	1.1 ± 0.5	1.5 ± 0.7	1.8 ± 1.2	0.002
ALT (IU/L)	17 (14–24)	32 (21–54)	57 (39–87)	<0.0001
AST (IU/L)	19 (15–22)	24 (18–33)	37 (27–51)	<0.0001
GGT (IU/L)	21 (13–50)	34 (21–81)	44 (27–78)	0.31
Steatosis ≥ 2 (yes), n (%)	0	66 (29)	156 (92)	<0.0001*
Lobular inflammation ≥ 1 (yes), n (%)	0	122 (53)	170 (100)	<0.0001*
Ballooning ≥ 1 (yes), n (%)	0	39 (17)	108 (64)	<0.0001*
Fibrosis ≥ 2 (yes), n (%)	0	7 (3)	81 (48)	<0.0001*
NAS > 5 (yes), n (%)	0	1 (0.4)	118 (70)	<0.0001*
FIB-4	0.72 ± 0.4	0.99 ± 0.8	1.33 ± 0.9	<0.0001*
CTSD (pg/mL)	3415 (1658–7371)	11,842 (1873–13,681)	13,047 (6512–14,268)	<0.0001

Note: Values are reported as mean ± SD or median (IQR) as appropriate.

Abbreviations: ALT, alanine aminotransferase; AST, aspartate aminotransferase; CTSD, circulating cathepsin D; F, female; FIB-4, fibrosis 4; GGT, gamma glutamyl transferase; HDL, high-density lipoprotein; IFG, impaired fasting; LDL, low-density lipoprotein; M, male; MASLD, metabolic dysfunction-associated steatotic liver disease; NAS, MASLD activity score; T2D, type 2 diabetes mellitus.

\*p value at  $\chi^2$  test.

## METHODS

### Study design and patient selection

Bulk RNA-seq analysis was performed in 167 individuals with obesity (Hepatic Transcriptomic cohort), of whom 125 hepatic samples were already available [9]. Adipose tissue from a subgroup of patients (n = 79) was also processed for RNA-seq (Adipose Transcriptomic cohort). The study included patients who underwent percutaneous liver and VAT biopsies performed during bariatric surgery at Fondazione IRCCS Cà Granda Ospedale Maggiore Policlinico (Milan, Italy). Exclusion criteria were applied as previously described [12]. According to the histological classification, the Hepatic Transcriptomic cohort included 29 patients with normal liver (C), 91 with mild MASLD (M), and 47 with severe MASLD (S), whereas the Adipose Transcriptomic cohort was composed of 16 patients with normal liver (C), 36 with mild MASLD (M), and 27 with severe MASLD (S) (Figure S1A). Study design and clinical features of enrolled patients are presented in Figure S1A and Table 1.

CTSD serum levels were retrospectively assessed in 52 patients with obesity belonging to the Hepatic Transcriptomic cohort. The association between circulating CTSD and liver damage was replicated in an independent cohort (Liver Clinic) of 432 patients with MASLD who underwent liver biopsies for suspected MASH at the Metabolic Diseases outpatient service at Fondazione IRCCS Cà Granda, Milan. Participants included in the Liver Clinic cohort were enrolled by

applying the aforementioned criteria [12]. Clinical features of the Liver Clinic cohort are summarized in Table 2.

Informed written consent was obtained from each patient, and the study protocol was approved by the Ethical Committees of Fondazione IRCCS Cà Granda Ospedale Maggiore Policlinico, Milan, and conformed to the 1975 Declaration of Helsinki (Ethics Committee no. 164\_2019).

### Transcriptomic and bioinformatic analysis

The detailed protocol for the transcriptomic analysis is provided in online Supporting Information. RNA was sequenced using the Illumina HiSeq4000 (Novogene Co., Guangzhou City, Guangdong Province, China). The quality of the reads was determined using FastQC software (Babraham Bioinformatics, Babraham, Cambridgeshire, UK), and low-quality sequences were trimmed using Cutadapt [13]. Reads were aligned to the human reference genome (GRCh38/hg38) using STAR [14]. Principal component analysis was calculated for transcript count matrix (see Supporting Information Results, Figure S1B,C).

To remove possible batch effect and unwanted sources of variation, we applied a surrogate variable analysis (SVA; version 3.35.2) [15]. The surrogate variables obtained as surrogate variable analysis-output were used as covariates to adjust for latent sources of noise in

differentially expressed gene (DEG) analysis. We defined DEGs as those with a *p* value corrected by Benjamini–Hochberg false discovery rate < 0.05 and fold change > |0|.

## Evaluation of circulating CTSD

Circulating levels of CTSD were assessed in duplicate by using Human Cathepsin(D) DuoSet ELISA kit (R&D Systems, Inc., Minneapolis, Minnesota) on serum samples collected at the time of liver biopsy in both the Hepatic Transcriptomic and Liver Clinic cohorts. The intra-assay coefficient of variation was <10%, whereas the inter-assay coefficient of variation was <12%.

## Statistics

For descriptive statistics, continuous variables were shown as mean and standard deviation (SD), whereas categorical variables were presented as number and proportion. Highly skewed biological variables were reported as median and interquartile range (IQR) and were log-transformed before analyses. Kruskal–Wallis or  $\chi^2$  tests were applied to test differences between non-categorical and categorical variables, respectively.

Multinomial logistic regression models were fit to examine binary traits (MASH, MASLD activity score [NAS] > 5), and ordinal regression models were fit for ordinal traits (stage of fibrosis). When specified, confounding factors were included in a model [16].

In the transcriptome analysis, *p* values were corrected for multiplicity by Benjamini–Hochberg method, and adjusted *p* < 0.05 were considered statistically significant. The description of transcriptomic analysis and adjusting factors is provided in online [Supporting Information](#). Statistical analyses were carried out using R software version 4.0.4 (<http://www.R-project.org>; R, Vienna, Austria) and JMP Pro version 16.1 (SAS Institute, Inc., Cary, North Carolina).

## RESULTS

### Gene signature and pathway-enriched analysis across MASLD severity

#### DEGs in hepatic and adipose tissues

Clinical features of the Hepatic and Adipose Transcriptomic cohorts (*n* = 167 and *n* = 79, respectively) are presented in Table 1 and online [Supporting Information](#) Results.

We performed a differential analysis to assess the liver transcriptome changes across disease severity. Compared to normal liver, a total of 227 genes (*n* = 59 upregulated and *n* = 168 downregulated) were differentially expressed in mild MASLD (i.e., mild MASLD vs. normal liver [MvC]; Table S1). Among the most upregulated, we found enolase 3 (*ENO3*), fibronectin type III domain containing 5 (*FNDC5*), SMAD family member 5 (*SMAD5*), tetraspanin 3 (*TSPAN3*),

and tyrosine kinase non receptor 2 (*TNK2*). Moreover, in this comparison, there were two highly expressed noncoding genes, mitochondrially encoded cytochrome C oxidase (MT-CO1) pseudogene 40 (*MTCO1P40*) and mitochondrially encoded 16S RNA like 12 pseudogene (*MTRNR2L12*; Figure 1A). The most downregulated DEGs were insulin-like growth factor 1 (*IGF1*), apolipoprotein F (*APOF*), aldehyde dehydrogenase 6 family member A1 (*ALDH6A1*), *ALDH18A1*, lysyl-tRNA synthetase 1 (*KARS1*), and the DIO3 opposite strand upstream RNA (*DIO3OS*) noncoding gene (Figure 1A).

In the severe MASLD versus normal liver (SvC) comparison, we found a total of 997 DEGs (*n* = 482 upregulated and *n* = 515 downregulated; Table S1). Genes with a higher expression were forkhead box N4 (*FOXN4*), *IL32*, *AKR1B10*, lysosomal associated membrane protein (*LAMP1/2/3*), matrix metalloproteinase 9 (*MMP9*), collagen type III  $\alpha$  1 chain (*COL3A1*), C-X-C motif chemokine ligand 9 (*CXCL9*), *CTSD*, *TSPAN3*, and *FNDC5*, whereas the downregulated ones were *APOF*, superoxide dismutase 1 (*SOD1*), sex hormone binding globulin (*SHBG*), *ALDH6A1*, complement 6 (*C6*), and *DIO3OS* (Figure 1B).

Concerning severe versus mild MASLD (SvM), we revealed 424 DEGs, with 281 being upregulated and 143 being downregulated (Table S1). The *AKR1B10*, *CSTD*, *IL32*, thrombospondin 1 (*THBS1*), *MMP9*, *CXCL8*, lysyl oxidase like 4 (*LOXL4*), *LAMP1/2/3*, microtubule associated protein 1 light chain 3  $\alpha$  (*MAP1LC3A*), transforming growth factor  $\beta$  3 (*TGFB3*), and *COL3A1/COL1A1* genes were upregulated, and most of them were shared with SvC, thereby suggesting that they may define a more severe condition. Notably, the expression of *FNDC5* progressively increased with disease severity. DEGs that were mostly downregulated in SvM were polycystin 2, transient receptor potential cation channel (*PKD2*), single-pass membrane protein with aspartate rich tail 1 (*SMDT1*), ubiquitin B (*UBB*), and *DIO3OS* (Figure 1C).

By exploiting a Venn diagram, we found that 128 genes mainly involved in complement activation, oxidative damage, and mitochondrial ribosomal assembly were deregulated in both mild and severe MASLD, suggesting an impairment of these processes in the early phases of the disease. Conversely, 214 genes that participate in autophagy and collagen deposition were featured in severe MASLD (Figure 1D).

We replicated the aforementioned differential analysis in VAT. Comparing MvC, we detected 28 DEGs (*n* = 14 upregulated and *n* = 14 downregulated; Table S1), and we highlighted an increased expression of aspartate  $\beta$ -hydroxylase (*ASPH*), integrin subunit  $\beta$  5 (*ITGB5*), Yes1 associated transcriptional regulator (*YAP1*), and palmdelphin (*PALMD*), whereas coenzyme Q8A (*COQ8A*), ATP binding cassette subfamily A member 10 (*ABCA10*), CD63 molecule (*CD63*), and electron transfer flavoprotein subunit  $\alpha$  (*ETFA*) were downregulated (Figure 1E).

In SvC, we found a total of 664 DEGs (*n* = 283 upregulated and *n* = 381 downregulated; Table S1). Among the most upregulated genes, there were *CXCL10*, secreted phosphoprotein 1 (*SPP1*), *MMP9*, chitinase 3 like 1 (*CHI3L1*), lipase A, lysosomal acid type (*LIPA*), NAD(P)H quinone dehydrogenase 1 (*NQO1*), leptin (*LEP*), and *ALDH4A1*. Notably, as previously described in obese mice and patients with MASLD, the *APOA4* antisense, which is considered a



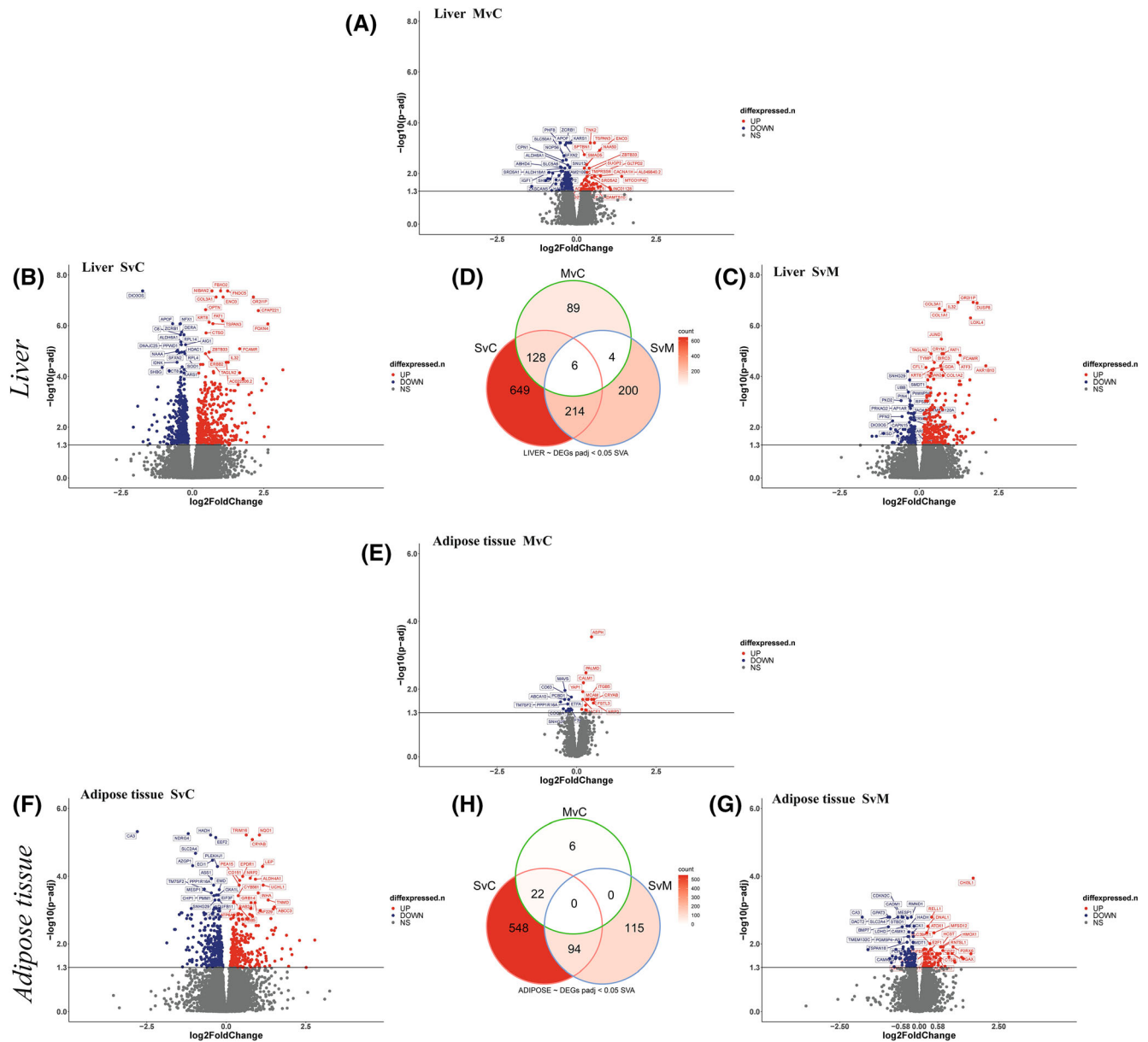


**FIGURE 1** Gene signature that characterizes mild and severe metabolic dysfunction-associated steatotic liver disease (MASLD) in liver and adipose tissue. Volcano plots illustrate the differentially expressed genes (DEGs) observed in the comparisons between (A) mild MASLD versus normal liver (MvC), (B) severe MASLD versus normal liver (SvC), and (C) severe versus mild MASLD (SvM) in liver. (D) Venn diagram showing common DEGs among MvC, SvC, and SvM. Volcano plots illustrate DEGs observed in (E) MvC, (F) SvC, and (G) SvM comparisons in adipose tissue. Venn diagram showing common DEGs among (H) MvC, SvC, and SvM. The x-axis shows the log<sub>2</sub> fold change, whereas the y-axis represents the  $-\log_{10}$  of *p* value adjusted (*p*-adj). Significantly downregulated DEGs are plotted in blue, upregulated DEGs in red, and non-significant DEGs in dark gray. The continuous line indicates the threshold of adjusted *p* < 0.05 above which significant DEGs are plotted. [Color figure can be viewed at [wileyonlinelibrary.com](http://wileyonlinelibrary.com)]

regulatory long noncoding RNA (lncRNA) of *APOA4*, has been found to be strongly upregulated [17]. Carbonic anhydrase 3 (*CA3*), hydroxyacyl-CoA dehydrogenase (*HADH*), *C6*, solute carrier family 2 member 4 (*SLC2A4*), NADH:ubiquinone oxidoreductase subunit B11 (*NDUFB11*), and *OXA1L* mitochondrial inner membrane protein (*OXA1L*) expression was reduced in SvC (Figure 1F).

Next, in SvM, we found a total of 209 DEGs (*n* = 86 upregulated and *n* = 123 downregulated; Table S1). *CHI3L1*, *CTSD*, *MMP9*, *APOC1*,

*LEP*, and heme oxygenase 1 (*HMOX1*) genes had the higher log<sub>2</sub> fold change, and some of them were shared with the previous comparison (SvC). The lower log<sub>2</sub> fold change was detected in *CA3*, adiponectin, *C1Q* and collagen domain containing (*ADIPOQ*), lactate dehydrogenase D (*LDHD*), required for meiotic nuclear division 1 homolog (*RMND1*), perilipin 5 (*PLIN5*), and *SLC2A4* (Figure 1G).

The Venn diagram showed that 22 genes mainly involved in adipogenesis, oxidative phosphorylation, and epithelial mesenchymal

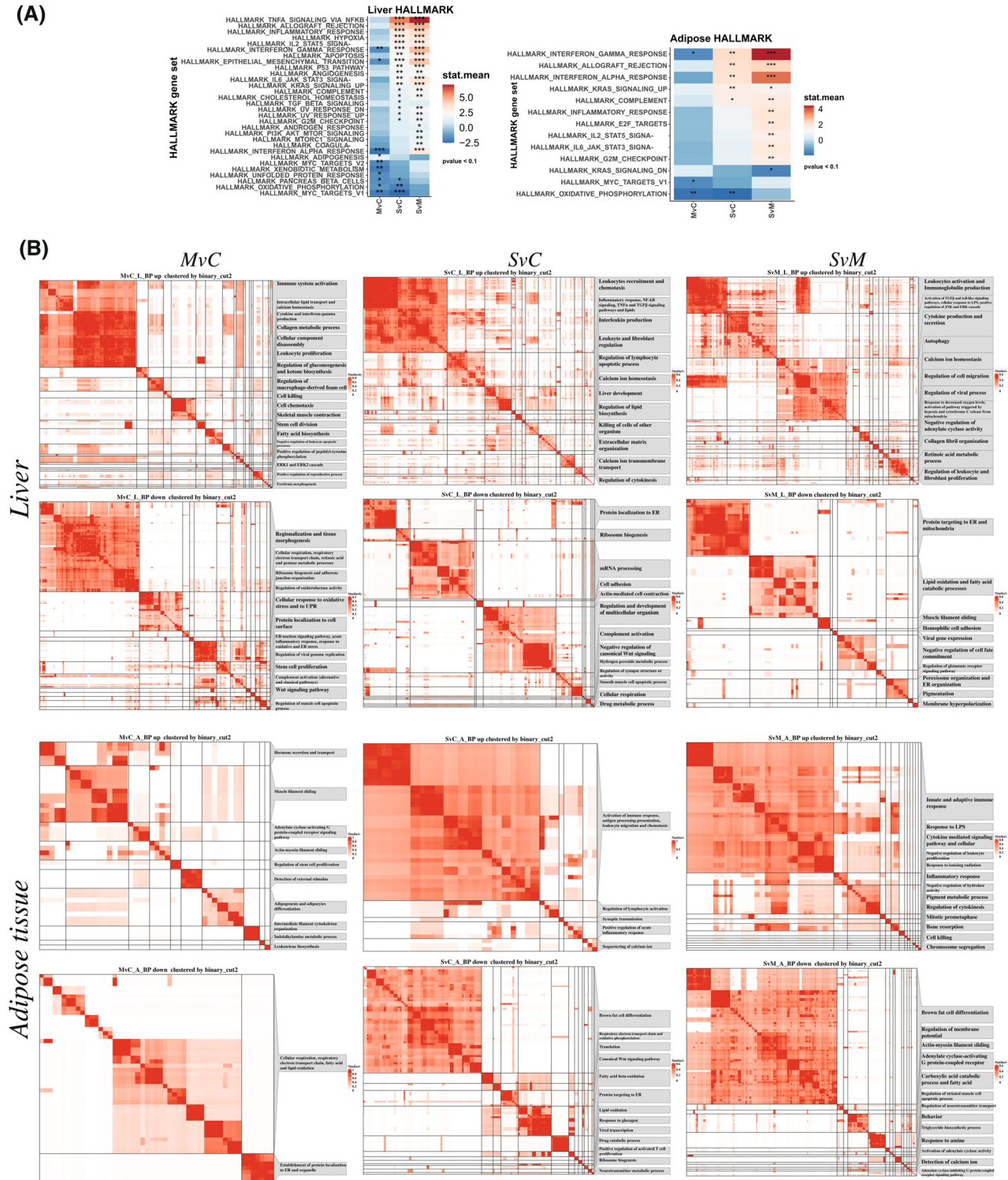


**FIGURE 2** Pathway and functional enrichment analysis of differentially expressed genes (DEGs) across metabolic dysfunction-associated steatotic liver disease (MASLD) stages in liver and adipose tissue. (A) Pathway-enriched analysis of DEGs in the comparisons among MASLD versus normal liver (MvC), severe MASLD versus normal liver (SvC), and severe versus mild MASLD (SvM) using HALLMARK data set in both liver (left) and adipose tissue (right). Red shading indicates induction, and blue shading indicates repression relative to the stat.mean (mean of gene set test statistics). \*p < 0.05, \*\*p < 0.01, and \*\*\*p < 0.001. (B) Gene ontology (GO) terms of the category biological processes (BP) in which DEGs are involved are clustered according to their similarity. Heat maps illustrate the upregulated GO-BP terms (top) and the downregulated ones (bottom) that clustered together by similarity index in liver (upper panel) and adipose tissue (lower panel) in the comparisons among MvC, SvC, and SvM. [Color figure can be viewed at [wileyonlinelibrary.com](https://onlinelibrary.wiley.com)]

transition (EMT) were deregulated in both mild and severe MASLD, whereas 94 genes were specifically associated with advanced disease and were related to autophagy, phosphoinositide 3-kinase (PI3K)/protein kinase B (Akt)/mammalian target of rapamycin (mTOR) signaling, adipogenesis, IR, and oxidative phosphorylation (Figure 1H).

### Pathway and functional enrichment analysis of DEGs across the disease stages

According to the HALLMARK data set, hepatic upregulated enriched pathways were tumor necrosis factor  $\alpha$  (TNF $\alpha$ ) signaling and inflammatory response, hypoxia, EMT, and apoptosis in SvM and more so in SvC (Figure 2A, left panel). Conversely, oxidative phosphorylation, unfolded protein response, and insulin activation were downregulated in MvC and SvC. Pathway-enriched analysis by the Kyoto Encyclopedia of Genes and Genomes (KEGG) confirmed HALLMARK results.

In VAT, interferon (IFN)- $\alpha$  and - $\gamma$  response and GTPase KRas signaling were upregulated in SvC and SvM. Inflammatory response, G2-M checkpoint, and transcription factor E2F targets were upregulated in SvM, whereas oxidative phosphorylation was downregulated in MvC and SvC (Figure 2A, right panel).

In liver, the key biological processes (gene ontology [GO] terms) that were upregulated in the MvC comparison were mainly involved in immune system activation, intracellular lipid transport and calcium homeostasis, collagen synthesis, gluconeogenesis, and ketogenesis. Among the downregulated ones, we found processes related to respiratory electron transport chain (ETC), response to oxidative and endoplasmic reticulum (ER) stress, and complement activation (Figure 2B, upper panel). Concerning SvC, the GO terms upregulated included leukocytes recruitment and chemotaxis, fibroblast proliferation and collagen production, and lipid synthesis and ECM organization, whereas those related to protein localization in ER and post-translational modifications were reduced (Figure 2B, upper panel). The upregulated GO terms that definitely discriminate SvM regard chronic leukocyte activation and immunoglobulin (Ig) production, TGF- $\beta$  and toll-like signaling pathways, response to hypoxia, autophagy, release of cytochrome C from mitochondria, positive regulation of c-Jun NH<sub>2</sub>-terminal kinase (JNK) and extracellular signal-regulated kinase (ERK) cascade, unfolded protein response, and organization of collagen fibers. Among the downregulated processes, we identified those associated with protein targeting to ER and mitochondria, lipid oxidation, and FA catabolism (Figure 2B, upper panel).

Concerning adipose tissue, the key biological processes that were upregulated in the MvC comparison were hormone secretion, adipogenesis, adipocyte differentiation, and leukotriene biosynthesis. Cellular respiration, FA oxidation, respiratory ETC, ribosome biogenesis, and protein localization in ER were reduced (Figure 2B, lower panel). In the SvC comparison, the antigen processing presentation, leukocyte proliferation, migration, and chemotaxis were increased, whereas the downregulated processes were brown fat cell differentiation, respiratory ETC, FA oxidation, protein targeting to ER, cellular response to glucagon, and ribosome biogenesis (Figure 2B, lower panel).

The upregulated GO terms that distinguish SvM were innate and adaptive immune response and cytokine mediated signaling pathway, whereas those involved in FA metabolism, brown fat cell differentiation, and triglyceride biosynthesis were reduced (Figure 2B, lower panel).

### Comparative analysis of DEGs to identify possible disease biomarkers

To identify the genes of interest (GoI) that may be featured in severe MASLD and that might be possibly used as biomarkers, we performed a comparative analysis of DEGs between liver and VAT, and we found 13 DEGs commonly deregulated in SvM (Figure 3A,B). Ribosomal protein S6 kinase A1 (*RPS6KA1*), ATPase H<sup>+</sup> transporting VO subunit b (*ATP6V0B*), cysteine rich transmembrane BMP regulator 1 (*CRIM1*), capping actin protein, gelsolin like (*CAPG*), nucleic acid binding protein 1 (*NABP1*), zinc finger matrin-type 3 (*ZMAT3*), *CTSD*, and *MMP9* genes were upregulated, whereas heat shock transcription factor 1 (*HSF1*), *UBB*, branched-chain amino acid transaminase 2 (*BCAT2*), and single-pass membrane protein with aspartate rich tail 1 (*SMDT1*) were downregulated. Notably, the 4-hydroxy-2-oxoglutarate aldolase 1 (*HOGA1*) gene had an opposite trend with a lower expression in liver and a higher one in adipose tissue in the severe condition (Figure 3C).

*SMDT1* is responsible for the Ca<sup>2+</sup> transport to the mitochondrial matrix, and it is localized in the inner membrane [18]. Ca<sup>2+</sup> homeostasis is essential for cell viability and to maintain mitochondrial function, and its regulation has been pointed to as a therapeutic target in MASLD. Similarly, another gene localized in mitochondria and downregulated in the severe condition was *BCAT2*, which catalyzes the first step of branched-chain amino acid synthesis [19]. In patients with advanced liver damage, plasma branched-chain amino acids decline and their supplementation alleviates steatosis and oxidative stress. *HOGA1* is involved in mitochondrial glyoxylate metabolism, which is altered in steatotic hepatocytes, thereby contributing to extrahepatic complications [20]. Conversely, a dysregulation of the *ATP6V0B*, *CTSD*, *UBB*, *RPS6KA1*, and *HSF1* genes may be representative of an impairment of the autophagy-lysosomal pathway, supporting the notion that these alterations boost advanced MASLD, as inferred by pathway analysis. In particular, *CTSD*, which emerged as an upregulated protein in the topological analysis of both tissues in severe conditions, is a lysosomal protease that impacts on lipid metabolism in patients with MASLD, and it has been associated with MASH development [21]. Finally, *ZMAT3*, *NABP1*, *CAPG*, and *CRIM1* genes are involved in apoptosis, programmed cell death, and cellular response to DNA damage.

We next applied a gene set variation analysis (GSVA) to build a score considering the integrated expression of these 13 genes (Figure 3D). GSVA scores discriminated SvM in both tissues ( $p < 0.05$ ), whereas there was not any difference in MvC. In receiver operating characteristic (ROC) analysis, the diagnostic accuracy in predicting severe MASLD was higher by combining all 13 genes weighted for alanine aminotransferase (ALT) and aspartate aminotransferase (AST; area under the curve [AUC] = 0.86 liver; AUC = 1.00 adipose)



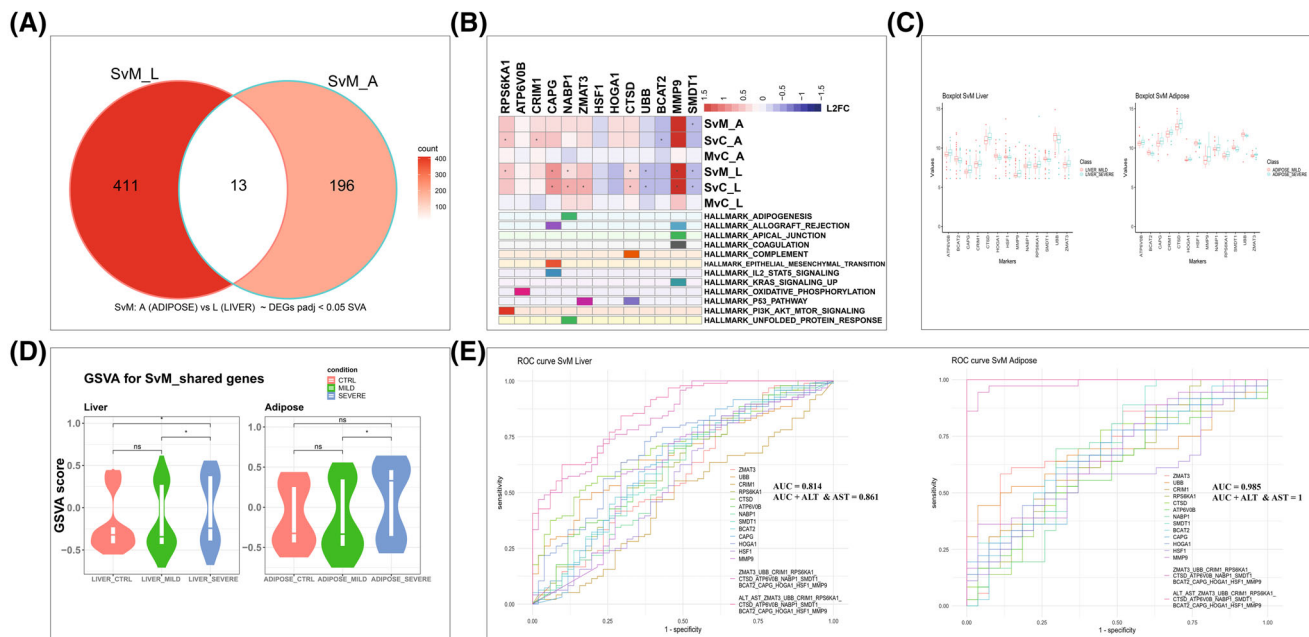


**FIGURE 3** Comparative analysis of differentially expressed genes (DEGs) to identify genes of interest (GoI). (A) Venn diagram shows the 13 common DEGs (adjusted  $p < 0.05$ ) in severe versus mild metabolic dysfunction-associated steatotic liver disease (MASLD; SvM) shared by liver and adipose tissue. (B) Heat map illustrates the expression of each DEG across the comparisons among mild MASLD versus normal liver (MvC), severe MASLD versus normal liver (SvC), and SvM in liver and adipose tissue. Red shading indicates induction, and blue shading indicates repression. The matrix below indicates the pathways by HALLMARK to which each gene belongs (dark color). (C) The expression of 13 common genes between liver and adipose tissue in the SvM comparison is stratified according to the severity of MASLD in both liver (left) and adipose tissue (right). Boxes span from the 25th to the 75th percentiles, whereas whiskers indicate the 10th and 90th percentiles. Mild MASLD is plotted in red, whereas severe MASLD is in blue. (D) Gene set variation analysis (GSEA) score of 13 common DEGs in normal liver (CTRL), mild and severe MASLD in liver (left), and in adipose tissue (right). \* $p < 0.1$ , \*\* $p < 0.01$ , and \*\*\* $p < 0.001$  at Student  $t$  test. (E) Receiver operating characteristic (ROC) curves of 13 common DEGs (adjusted  $p < 0.05$ ) in SvM shared by liver (left) and adipose tissue (right), obtained considering each gene alone or 13 genes combined in a generalized linear model weighted or not for alanine aminotransferase (ALT) and aspartate aminotransferase (AST). Area under the curves (AUC) reported in the graph. [Color figure can be viewed at [wileyonlinelibrary.com](http://wileyonlinelibrary.com)]

or not (AUC = 0.84 liver; AUC = 0.98 adipose; Figure 3E, online Supporting Information Results).

### Serum CTSD may be used as a biomarker to diagnose severe MASLD

Although several circulating molecules have been proposed as biomarkers for advanced disease, no one, to our knowledge, has obtained a recognized clinical consensus. Therefore, we decided to focus our attention on those genes that encode for secreted proteins that have been identified in SvM and confirmed in SvC. Among them, the gene with the higher counts and AUC in predicting severe MASLD in both hepatic and adipose tissue was CTSD, a member of the autophagy-lysosomal pathway. We observed that CTSD expression was higher in severe MASLD compared with control and mild disease in both tissues (Figure 4A,B). These data were corroborated in publicly available data sets, including GSE126848 [22] and GSE135251 [10].

In addition, to assess the diagnostic efficacy of CTSD, we built a ROC curve by considering it alone or combined with ALT and

AST, which represent the most common noninvasive parameters of liver damage. In ROC curve analysis, the AUC weighted for ALT and AST was 0.78 in liver and 0.76 in VAT for SvM, whereas it was 0.87 and 0.88, respectively, for SvC, thus suggesting that CTSD combined with transaminases better predicts the severe status (Figure 4C–F).

Then, to validate these findings, we assessed CTSD serum levels in  $n = 432$  patients with histological diagnosis of MASH (Liver Clinic cohort) who are not affected by severe obesity. Serum CTSD progressively increased from normal liver to severe MASLD, thereby confirming the data observed in the Transcriptomic cohorts (adjusted  $p = 0.001$  SvC and adjusted  $p = 0.0006$  SvM; Figure 5A). By weighting circulating CTSD for ALT and AST, we obtained that the AUC was 0.78 and 0.87 in SvM and SvC, respectively, thus confirming its higher diagnostic performance in advanced disease when combined with transaminases (Figure 5B,C). In multivariate analysis, adjusted for sex, age, body mass index (BMI), and type 2 diabetes mellitus, circulating CTSD was associated with steatosis, lobular inflammation, fibrosis, MASH, and MASLD activity score (NAS) > 5 (Table S2).

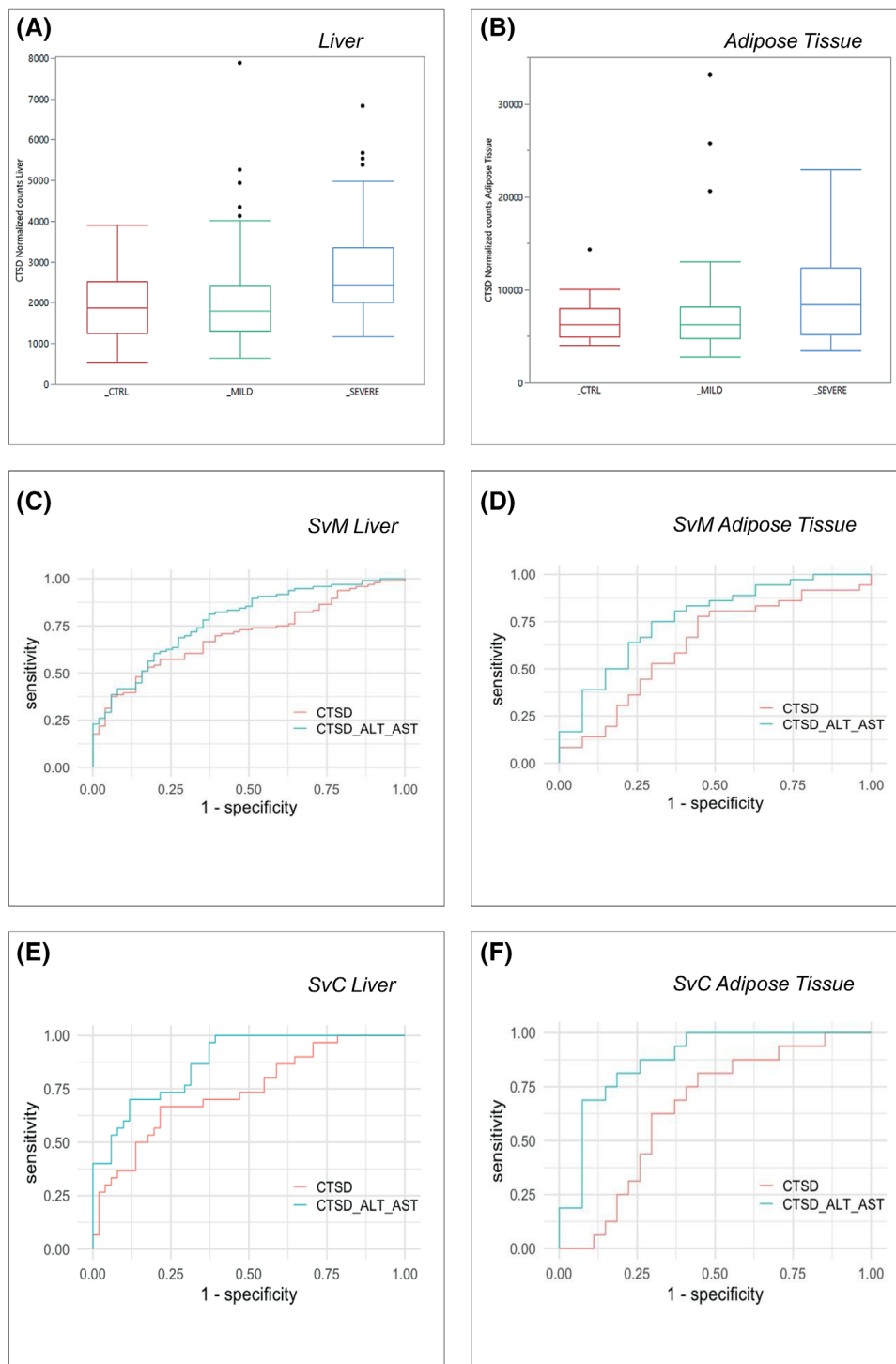


**FIGURE 4** Hepatic and adipose tissue cathepsin D (CTSD) is increased in severe metabolic dysfunction-associated steatotic liver disease (MASLD). CTSD expression is stratified according to the severity of MASLD in both (A) liver and (B) adipose tissue. Boxes span from the 25th to the 75th percentiles, whereas whiskers indicate the 10th and 90th percentiles. Normal liver (CTRL) is plotted in red and mild in green, whereas severe MASLD is in blue. Receiver operating characteristic (ROC) curves describe the accuracy of (C, E) hepatic and (D, F) adipose tissue gene expression of CTSD in foreseeing severe versus mild MASLD (SvM) and severe MASLD versus normal liver (SvC), respectively. ROC curves were obtained considering CTSD alone or in a generalized linear model weighted for alanine aminotransferase (ALT) and aspartate aminotransferase (AST). Area under the curves (AUCs) reported in the graphs. [Color figure can be viewed at [wileyonlinelibrary.com](https://onlinelibrary.wiley.com/doi/10.1111/obes.12500)]

Finally, we tried to compare the diagnostic accuracy of CTSD with that of FIB-4, a noninvasive tool of fibrosis that is largely used in MASLD and the calculation of which takes into account transaminase

levels. FIB-4 is usually suggested to be used considering the lower threshold of 1.3 as absence and the higher threshold than 2.67 as presence of fibrosis. However, the indeterminate values

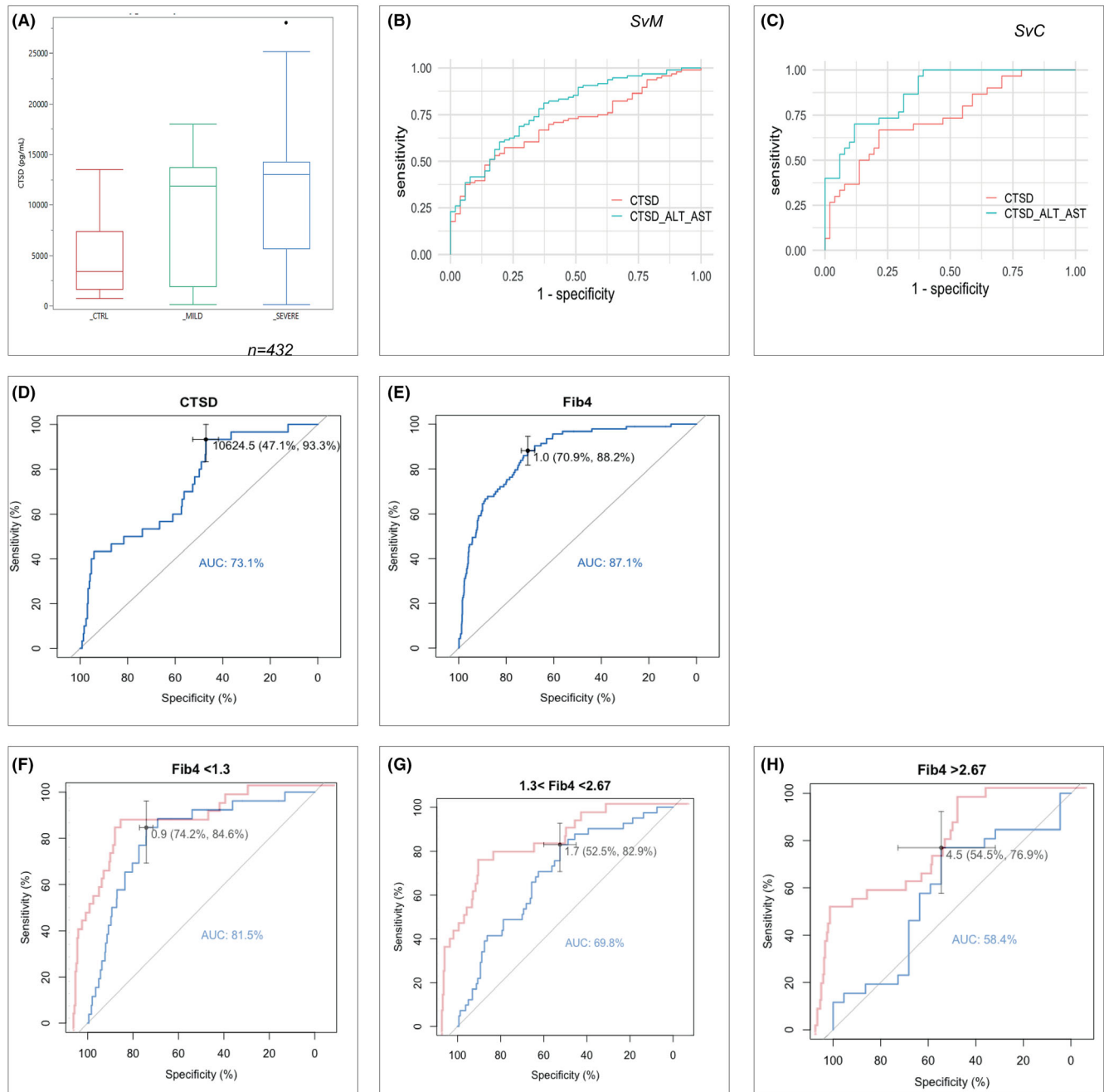


**FIGURE 5** Serum cathepsin D (CTSD) as possible biomarker to detect severe metabolic dysfunction-associated steatotic liver disease (MASLD). (A) Serum CTSD was assessed in  $n = 432$  patients (Liver Clinic cohort) with histological diagnosis of metabolic dysfunction-associated steatohepatitis (MASH), enrolled at the Metabolic Diseases outpatient service.  $P < 0.05$  at one-way ANOVA. Receiver operating characteristic (ROC) curves describe the accuracy of circulating CTSD (picograms per milliliter) in foreseeing (B) severe versus mild MASLD (SvM) and (C) severe MASLD versus normal liver (SvC), obtained considering CTSD alone or in a generalized linear model with transaminases (alanine aminotransferase [ALT] and aspartate aminotransferase [AST]). Area under the curves (AUC) reported in the graphs. ROC curves describe the accuracy of (D) serum CTSD (picograms per milliliter) and (E) fibrosis 4 (FIB-4) in predicting MASH fibrosis. FIB-4 values were subdivided in the following three categories:  $<1.3$ ,  $1.3$  to  $2.67$ , and  $>2.67$ . (F–H) ROC curves describe the accuracy of serum CTSD combined with the three categories of FIB-4 (red line) compared with the latter alone in predicting MASH fibrosis (blue line). [Color figure can be viewed at [wileyonlinelibrary.com](http://wileyonlinelibrary.com)]

( $1.3 < \text{FIB-4} < 2.67$ ) fall into a “gray area” in which patients are characterized by an intermediate risk of fibrosis, although these are considered nondiagnostic results. Therefore, this area needs to be further investigated.

To this purpose, we evaluated whether circulating CTSD may improve the accuracy of FIB-4 in the gray area in detecting MASH with fibrosis, and we found that AUC rises from  $0.69$  to  $0.84$  (Figure 5D–H).

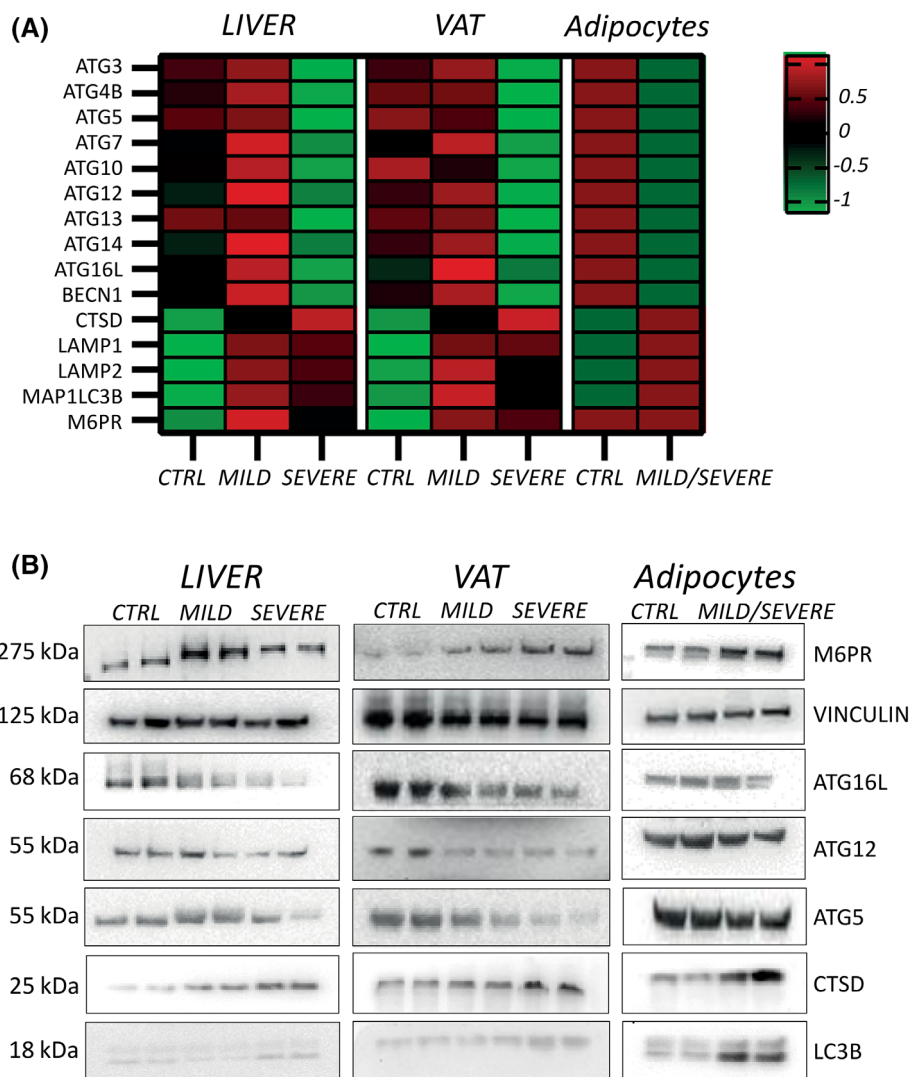


**FIGURE 6** Hepatic and visceral adipose tissue (VAT) autophagy-lysosomal pathway is impaired in severe metabolic dysfunction-associated steatotic liver disease (MASLD). (A) The heat map represents the expression of genes involved in the autophagy-lysosomal pathway in hepatic and VAT samples from  $n = 20$  patients with obesity stratified according to disease severity and in primary adipocytes isolated from a subgroup ( $n = 10$ ) of VAT samples. mRNA values were assessed by quantitative real-time polymerase chain reaction (qRT-PCR), and data were normalized on  $\beta$ -actin as housekeeping gene. (B) Western blot analysis was performed in hepatic and VAT samples from  $n = 20$  patients with obesity stratified according to disease severity and in primary adipocytes isolated from a subgroup ( $n = 10$ ) of VAT samples. Proteins of patients who belong to the same group were pooled and protein levels were normalized on vinculin as housekeeping. [Color figure can be viewed at [wileyonlinelibrary.com](https://onlinelibrary.wiley.com/doi/10.1111/ob.14700)]

### Increased CTSD expression is associated with reduced autophagy

Next, we sought to further characterize the role of CTSD in promoting advanced disease by investigating the autophagy-lysosomal pathway in a small cohort of bariatric patients ( $n = 20$ ) for whom matched hepatic and adipose tissues were available (Tables S3 and S4). In the severe condition, both tissues showed a downregulation of mRNA levels of the autophagy-related (ATG) family involved in autophagic processes. Conversely, markers of endo-lysosomal function, including CTSD, were increased, suggesting an overall increase in lysosomal mass possibly in the attempt to compensate for the block of the autophagic fluxes (Figure 6A).

For protein levels, mannose-6-phosphate receptor (M6PR), which is required for CTSD maturation/secretion and its shuttle from ER into

lysosomes, the mature form of CTSD, as well as the autophagy marker LC3B, one of the mammalian autophagy-related 8 (Atg8) homologs, was higher in severe MASLD in both tissues. Conversely, ATG16L, ATG5, and ATG12, essential for autophagosome formation, were decreased, thereby suggesting an impairment of autophagosomes' turnover during the progression from mild to advanced disease (Figure 6B). These results were confirmed in  $n = 10$  primary adipocytes obtained from the aforementioned patients (Figure 6A,B).

### DISCUSSION

In this study, we compared the hepatic and VAT transcriptomic profiles from histologically healthy liver to mild and severe MASLD with the purpose of identifying common deregulated pathways and shared



biomarkers that may be easily measured in sera, thus allowing the diagnosis of advanced disease.

We performed RNA-seq of 167 hepatic samples and 79 matched adipose tissues derived from adult patients with severe obesity, which represents one of the main risk factors of progressive MASLD. Although previous studies have explored the hepatic transcriptome in individuals with obesity [9, 23], the novelty of our study was in comparing the expression profile of both tissues to highlight the mechanisms by which VAT promotes MASH fibrosis.

In the attempt to identify a specific transcriptomic signature that may discriminate patients with mild and severe MASLD, we found 424 deregulated genes in liver, with 281 being upregulated and 143 being downregulated. Consistent with previous findings, the *AKR1B10*, *FNDC5*, *MMP9*, *LOXL4*, *IL32*, and *COL3A1/COL1A1* genes were upregulated, suggesting that they might define the presence of severe MASLD [9, 10]. In VAT, the DEGs between mild and severe MASLD were 209, and, among the most upregulated ( $n = 86$ ), we found *MMP9*, *LEP*, and genes involved in lipid metabolism, thereby reinforcing the pivotal role of expanded fat mass in prompting MASLD.

According to pathway analysis, inflammation, autophagy, ECM remodeling, and mitochondrial dysfunction were upregulated, whereas oxidative phosphorylation was downregulated in both tissues, thereby corroborating the relevance of these processes in the switching toward progressive MASLD. Notably, we first highlighted that the pathological events that occur in VAT may mirror those that feature in liver in the context of progressive MASLD and vice versa.

Next, to identify genes that may define severe MASLD and that could be possibly used as biomarkers, we performed a comparative DEG analysis revealing 13 commonly deregulated genes involved in EMT, inflammatory processes, apoptosis, and autophagy. Moreover, we built a GSVA score to predict MASLD severity in both tissues, taking into account the transcriptomic profile of overall genes. In ROC curve analysis, the highest diagnostic accuracy has been achieved by combining the expression of all 13 genes and more so after adjustment for ALT and AST.

To date, there is not a secreted noninvasive biomarker to discriminate advanced MASLD from simple steatosis. Although several of the molecules included in our 13-gene signature might be potential serum markers, we focused our attention on CTSD, a lysosomal-secreted protease that had the highest gene counts and accuracy in predicting severe histological MASLD in both tissues. CTSD, which is mainly expressed in immune cells, has been previously associated with MASH development [21, 24]. Indeed, it seems to be regulated in a timely manner in infiltrating and liver-resident cells depending on the cellular demands during MASLD progression. Therefore, it may participate in several biological processes such as inflammation, lipid metabolism, autophagy, ECM remodeling, fibrogenesis, and apoptosis.

In preclinical models, CTSD expression increases during hepatic stellate cell activation, and this upregulation occurs largely in lysosomes, although a significant fraction is secreted in the extracellular

media. The colocalization of cathepsins with markers of early and late endosomes indicates that their release follows the secretory pathway to potentially modulate ECM components, smooth muscle  $\alpha$ -actin ( $\alpha$ SMA), and TGF- $\beta$ . The latter are negatively modulated by CTSD downregulation, thereby suggesting that it directly impacts on hepatic stellate cell trans-differentiation and activation, which are critical steps of liver fibrogenesis [25]. Moreover, CTSD serum levels were found to be increased in patients with liver cirrhosis compared with steatosis, proposing that its collagenolytic activity may foster tissue remodeling and disease progression [26, 27]. Finally, plasma CTSD activity has also been positively correlated with type 2 diabetes mellitus and IR, which are the main drivers of progressive MASLD [28, 29].

It has been demonstrated that the pharmacological inhibition of CTSD improves dyslipidemia and promotes the switch of immune status toward an anti-inflammatory profile in preclinical models of MASH [30]. According to this evidence, we observed a higher CTSD expression in severe MASLD compared with the mild condition and normal liver. To verify whether the tissues' expression reflected CTSD circulating levels, we measured them in patients belonging to the Transcriptomic cohorts, and we found that the mRNA levels positively correlated with serum ones. We further corroborated these findings in the Liver Clinic cohort, and we observed that CTSD levels raised across disease severity, even irrespective of BMI, thereby extending its clinical utility even in patients without severe obesity.

Although CTSD has been previously associated with MASLD, it had never emerged as a shared gene between liver and VAT. To add a further message, we hypothesized its use in improving the diagnostic accuracy of FIB4 by focusing on the gray window in which the detection of fibrosis is uncertain. Specifically, we demonstrated that, by combining circulating CTSD with FIB-4 ranging from 1.3 to 2.67, the AUC was higher compared with FIB-4 alone in predicting MASH fibrosis. Indeed, in our cohort out of 30 patients with MASH fibrosis of whom serum CTSD was available, 21 (70%) fall in the gray area, and, according to the current approved cutoff, their diagnosis would not be correct.

Finally, we first also evaluated the functional role of CTSD in progressive disease by investigating the expression of lysosomal and autophagy-related mediators. We demonstrated that endo-lysosomal markers along with CTSD are boosted with the progression of MASLD in hepatic and VAT samples derived from bariatric patients whose clinical features mirror those of the Transcriptomic cohorts and in primary adipocytes. Conversely, markers implicated in autophagic machinery regulation are strongly suppressed. These data are in line with the previous evidence that has outlined an impairment of autophagolysosomal fluxes in experimental and clinical models of MASLD [31, 32]. The upregulation of lysosomal genes might be explained as a consequence of the increased lysosomal mass in an attempt to counteract lysosomal dysfunction due to lipid and cholesterol accumulation. In turn, lysosome engulfment has been shown to inhibit autophagosome turnover and impede the fusion between autophagosomes and lysosomes, thereby fostering defective autophagic clearance and multivesicular bodies buildup [33, 34].

In conclusion, we compared the transcriptomic profile of hepatic and adipose tissues in adult patients with severe obesity-related MASLD, identifying CTSD as a shared biomarker of autophagic impairment, the hepatic and circulating levels of which increase, paralleling the disease severity. Therefore, CTSD might represent an easily measurable biomarker to discriminate advanced disease from mild disease, possibly reinforcing the accuracy of FIB-4.<sup>10</sup>

## AUTHOR CONTRIBUTIONS

The authors' responsibilities were as follows: Marica Meroni, study design, data analysis and interpretation, and manuscript drafting; Emilia De Caro, Federica Chiappori, Ettore Mosca, Ivan Merelli, Alessandro Orro, and Alessandra Mezzelani, data analysis; Miriam Longo and Erika Paolini, data generation; Rosa Lombardi, Sara Badiali, and Marco Maggioni, patient recruitment and characterization; Luca Valenti and Anna Ludovica Fracanzani, contribution to discussion and manuscript revision; Paola Dongiovanni, study design, manuscript drafting, data analysis and interpretation, funding acquisition, and supervision and has primary responsibility for final content. All authors read and approved the final manuscript.

## FUNDING INFORMATION

This study was supported by Italian Ministry of Health (Ricerca Corrente 2024 – Fondazione IRCCS Cà Granda Ospedale Maggiore Policlinico), by Italian Ministry of Health (Finalized Research Ministry of Health GR-2019-12370172; RF-2021-12374481), and by 5x1000 2020 RC5100020B.

## CONFLICT OF INTEREST STATEMENT

The authors declared no conflict of interest.

## ORCID

Paola Dongiovanni  <https://orcid.org/0000-0003-4343-7213>

## REFERENCES

- Lazarus JV, Mark HE, Villota-Rivas M, et al. The global NAFLD policy review and preparedness index: are countries ready to address this silent public health challenge? *J Hepatol*. 2022;76:771-780.
- Francque SMA, Dirinck E. NAFLD prevalence and severity in overweight and obese populations. *Lancet Gastroenterol Hepatol*. 2023;8:2-3.
- Polyzos SA, Kountouras J, Mantzoros CS. Obesity and nonalcoholic fatty liver disease: from pathophysiology to therapeutics. *Metabolism*. 2019;92:82-97.
- Younossi ZM, Koenig AB, Abdelatif D, Fazel Y, Henry L, Wymer M. Global epidemiology of nonalcoholic fatty liver disease-meta-analytic assessment of prevalence, incidence, and outcomes. *Hepatology*. 2016;64:73-84.
- Meroni M, Longo M, Rustichelli A, Dongiovanni P. Nutrition and genetics in NAFLD: the perfect Binomial. *Int J Mol Sci*. 2020;21:21.
- Kouroumalis E, Voumvouraki A, Augoustaki A, Samonakis DN. Autophagy in liver diseases. *World J Hepatol*. 2021;13:6-65.
- Dongiovanni P, Stender S, Pietrelli A, et al. Causal relationship of hepatic fat with liver damage and insulin resistance in nonalcoholic fatty liver. *J Intern Med*. 2018;283:356-370.
- Guerra S, Mocciaro G, Gastaldelli A. Adipose tissue insulin resistance and lipidome alterations as the characterizing factors of non-alcoholic steatohepatitis. *Eur J Clin Invest*. 2022;52:e13695.
- Baselli GA, Dongiovanni P, Ramesta R, et al. Liver transcriptomics highlights interleukin-32 as novel NAFLD-related cytokine and candidate biomarker. *Gut*. 2020;69:1855-1866.
- Govaere O, Cockell S, Tiniakos D, et al. Transcriptomic profiling across the nonalcoholic fatty liver disease spectrum reveals gene signatures for steatohepatitis and fibrosis. *Sci Transl Med*. 2020;12:12.
- Sheldon RD, Kanosky KM, Wells KD, et al. Transcriptomic differences in intra-abdominal adipose tissue in extremely obese adolescents with different stages of NAFLD. *Physiol Genomics*. 2016;48:897-911.
- Meroni M, Longo M, Paolini E, et al. MAFLD definition underestimates the risk to develop HCC in genetically predisposed patients. *J Intern Med*. 2022;291:374-376.
- Martin M. Cutadapt removes adapter sequences from high-throughput sequencing reads. *EMBnet J*. 2011;17:10-12.
- Dobin A, Davis CA, Schlesinger F, et al. STAR: ultrafast universal RNA-seq aligner. *Bioinformatics*. 2013;29:15-21.
- Leek JT. Svsseq: removing batch effects and other unwanted noise from sequencing data. *Nucleic Acids Res*. 2014;42:e161.
- Konishi K, Miyake T, Furukawa S, et al. Advanced fibrosis of non-alcoholic steatohepatitis affects the significance of lipoprotein(a) as a cardiovascular risk factor. *Atherosclerosis*. 2020;299:32-37.
- Qin W, Li X, Xie L, et al. A long non-coding RNA, APOA4-AS, regulates APOA4 expression depending on HuR in mice. *Nucleic Acids Res*. 2016;44:6423-6433.
- Xie KF, Guo DD, Luo XJ. SMDT1-driven change in mitochondrial dynamics mediate cell apoptosis in PDAC. *Biochem Biophys Res Commun*. 2019;511:323-329.
- Lo EKK, Felicianna XJH, Zhan Q, Zeng Z, El-Nezami H. The emerging role of branched-chain amino acids in liver diseases. *Biomedicine*. 2022;10:1444.
- Gianmoena K, Gasparoni N, Jashari A, et al. Epigenomic and transcriptional profiling identifies impaired glyoxylate detoxification in NAFLD as a risk factor for hyperoxaluria. *Cell Rep*. 2021;36:109526.
- Ruiz-Blázquez P, Pistorio V, Fernández-Fernández M, Moles A. The multifaceted role of cathepsins in liver disease. *J Hepatol*. 2021;75:1192-1202.
- Suppli MP, Rigbolt KTG, Veidal SS, et al. Hepatic transcriptome signatures in patients with varying degrees of nonalcoholic fatty liver disease compared with healthy normal-weight individuals. *Am J Physiol Gastrointest Liver Physiol*. 2019;316:G462-G472.
- Subudhi S, Drescher HK, Dichtel LE, et al. Distinct hepatic gene-expression patterns of NAFLD in patients with obesity. *Hepatol Commun*. 2022;6:77-89.
- Walenbergh SM, Houben T, Rensen SS, et al. Plasma cathepsin D correlates with histological classifications of fatty liver disease in adults and responds to intervention. *Sci Rep*. 2016;6:38278.
- Moles A, Tarrats N, Fernández-Checa JC, Mari M. Cathepsins B and D drive hepatic stellate cell proliferation and promote their fibrogenic potential. *Hepatology*. 2009;49:1297-1307.
- Walenbergh SM, Houben T, Hendriks T, et al. Plasma cathepsin D levels: a novel tool to predict pediatric hepatic inflammation. *Am J Gastroenterol*. 2015;110:462-470.
- Leto G, Tumminello FM, Pizzolanti G, et al. Cathepsin D serum mass concentrations in patients with hepatocellular carcinoma and/or liver cirrhosis. *Eur J Clin Chem Clin Biochem*. 1996;34:555-560.
- Ding L, De Munck TJI, Oligschlaeger Y, et al. Insulin resistance is positively associated with plasma cathepsin D activity in NAFLD patients. *Biomol Concepts*. 2021;12:110-115.
- Ding L, Houben T, Oligschlaeger Y, et al. Plasma cathepsin D activity rather than levels correlates with metabolic parameters of type 2 diabetes in male individuals. *Front Endocrinol (Lausanne)*. 2020;11:575070.

30. Houben T, Oligschlaeger Y, Hendriks T, et al. Cathepsin D regulates lipid metabolism in murine steatohepatitis. *Sci Rep.* 2017;7:3494.
31. Carotti S, Aquilano K, Zalfa F, et al. Lipophagy impairment is associated with disease progression in NAFLD. *Front Physiol.* 2020;11:850.
32. Fukuda T, Ewan L, Bauer M, et al. Dysfunction of endocytic and autophagic pathways in a lysosomal storage disease. *Ann Neurol.* 2006;59:700-708.
33. Sarkar S, Carroll B, Buganim Y, et al. Impaired autophagy in the lipid-storage disorder Niemann-pick type C1 disease. *Cell Rep.* 2013;5:1302-1315.
34. Du J, Ji Y, Qiao L, Liu Y, Lin J. Cellular endo-lysosomal dysfunction in the pathogenesis of non-alcoholic fatty liver disease. *Liver Int.* 2020;40:271-280.

## SUPPORTING INFORMATION

Additional supporting information can be found online in the Supporting Information section at the end of this article.

**How to cite this article:** Meroni M, De Caro E, Chiappori F, et al. Hepatic and adipose tissue transcriptome analysis highlights a commonly deregulated autophagic pathway in severe MASLD. *Obesity (Silver Spring)*. 2024;32(5):923-937. doi:[10.1002/oby.23996](https://doi.org/10.1002/oby.23996)